EDGE ARTICLE

Check for updates

Hydrogen generation from methanol at near-room temperature†

Yangbin Shen,[ab] Yulu Zhan,[a] Shuping Li,[a] Fandi Ning,[a] Ying Du,[a] Yunjie Huang,[c] Ting He[a] and Xiaochun Zhou [ID] *[ad]

As a promising hydrogen storage medium methanol has many advantages such as a high hydrogen content (12.5 wt%) and low-cost. However, conventional methanol–water reforming methods usually require a high temperature (>200 °C). In this research, we successfully designed an effective strategy to fully convert methanol to hydrogen for at least 1900 min (~32 h) at near-room temperature. The strategy involves two main procedures, which are $CH_3OH \rightarrow HCOOH \rightarrow H_2$ and $CH_3OH \rightarrow NADH \rightarrow H_2$. HCOOH and the reduced form of nicotinamide adenine dinucleotide (NADH) are simultaneously produced through the dehydrogenation of methanol by the cooperation of alcohol dehydrogenase (ADH) and aldehyde dehydrogenase (ALDH). Subsequently, HCOOH is converted to H_2 by a new iridium polymer complex catalyst and an enzyme mimic is used to convert NADH to H_2 and nicotinamide adenine dinucleotide (NAD^+). NAD^+ can then be reconverted to NADH by repeating the dehydrogenation of methanol. This strategy and the catalysts invented in this research can also be applied to hydrogen production from other small organic molecules (e.g. ethanol) or biomass (e.g. glucose), and thus will have a high impact on hydrogen storage and applications.

1. Introduction

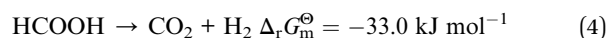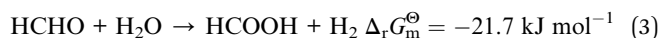Methanol is a promising hydrogen source because of its advantages of a high hydrogen content (12.5 wt%), low-cost and availability from biomass and chemical methods.[1–6] However, hydrogen production through the conventional methanol–water reforming reaction (reaction (1))[7–9] usually requires a high temperature (>200 °C)[10] and produces high concentrations of CO.[11–13] Trace CO (as low as 100 ppm) can poison the Pt catalyst in proton exchange membrane fuel cells (PEMFCs). This makes it difficult to use conventional reforming method in portable applications such as hydrogen vehicles.

$$CH_3OH + H_2O \rightarrow 3H_2 + CO_2 \; \Delta_r G_m^\Theta = 9.0 \text{ kJ mol}^{-1} \quad (1)$$
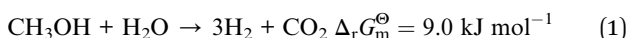
The whole reforming reaction can be divided into three main steps of simple reactions, labelled as reactions (2)–(4).[7–9,14,15] Of the three, reaction (2), the first step in methanol dehydrogenation, is the most difficult because it is an up-hill reaction ($\Delta_r G_m^\Theta > 0$). The following steps of formaldehyde and formic acid dehydrogenations in reactions (3) and (4) are much easier because they are down-hill reactions ($\Delta_r G_m^\Theta < 0$). The up-hill reaction (2) causes difficulty for the overall methanol–water reforming reaction even though the following steps can be catalyzed with a high reaction rate at low temperature.[16–20]

$$CH_3OH \rightarrow HCHO + H_2 \; \Delta_r G_m^\Theta = 63.7 \text{ kJ mol}^{-1} \quad (2)$$

$$HCHO + H_2O \rightarrow HCOOH + H_2 \; \Delta_r G_m^\Theta = -21.7 \text{ kJ mol}^{-1} \quad (3)$$

$$HCOOH \rightarrow CO_2 + H_2 \; \Delta_r G_m^\Theta = -33.0 \text{ kJ mol}^{-1} \quad (4)$$

To produce hydrogen from methanol at a low temperature (<100 °C), researchers recently invented some highly active and selective complex catalysts to catalyze methanol–water reforming at a low temperature (<100 °C) and produce high quality H_2 with only a trace of, or even completely without CO.[21–23] With this method, alkaline reagents as consumptive additives were usually added to the reaction system to achieve a high activity.[9,21,24–27] However, the acidic gas CO_2 from methanol reforming is able to neutralize the alkaline solution. Moreover, the reaction temperature was relatively high (~70 °C).

In order to allow the reforming process to occur at lower temperatures, an enzyme (oxidase) was used to partially oxidize methanol to formaldehyde using oxygen (also a consumptive additive) and then the formaldehyde was reformed with water to

aDivision of Advanced Nanomaterials, Suzhou Institute of Nano-tech and Nano-bionics, Chinese Academy of Sciences, Suzhou 215125, China. E-mail: xczhou2013@sinano.ac.cn

bUniversity of Chinese Academy of Sciences, Beijing 100049, China

cFaculty of Materials Science and Chemistry, China University of Geosciences, Wuhan 430074, China

dKey Laboratory of Nanodevices and Applications, Suzhou Institute of Nano-tech and Nano-bionics, Chinese Academy of Sciences, Suzhou 215125, China

† Electronic supplementary information (ESI) available. See DOI: 10.1039/c7sc01778b

generate hydrogen and CO_2 using ruthenium complexes (reaction (5)).[28]

$$CH_3OH + (1/2)O_2 \rightarrow 2H_2 + CO_2 \quad \Delta_r G_m^\ominus = -228.1 \text{ kJ mol}^{-1} \quad (5)$$

This process demonstrates an effective way to produce hydrogen from methanol at room temperature and under mild conditions. However, this method needs oxygen, which creates two serious disadvantages: low efficiency and danger. As shown in reaction (5), 1 methanol molecule in this reaction can only produce 2 hydrogen molecules but not 3 as in reaction (1). In addition, the mixture of oxygen and the produced hydrogen is very dangerous for mass production.

Until recently, it has still been a very challenging task to fully convert methanol to hydrogen at near-room temperature. However, in this research, we have successfully designed a strategy to overcome this challenge (Scheme 1a). With this strategy, dehydrogenases are used to dehydrogenate methanol to HCOOH, and the hydrogen from methanol is deposited in the reduced form of nicotinamide adenine dinucleotide (NADH). Then, hydrogen is generated from the decomposition of HCOOH and the dehydrogenation of NADH.
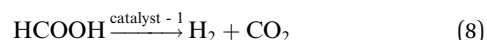
2. Results and discussion
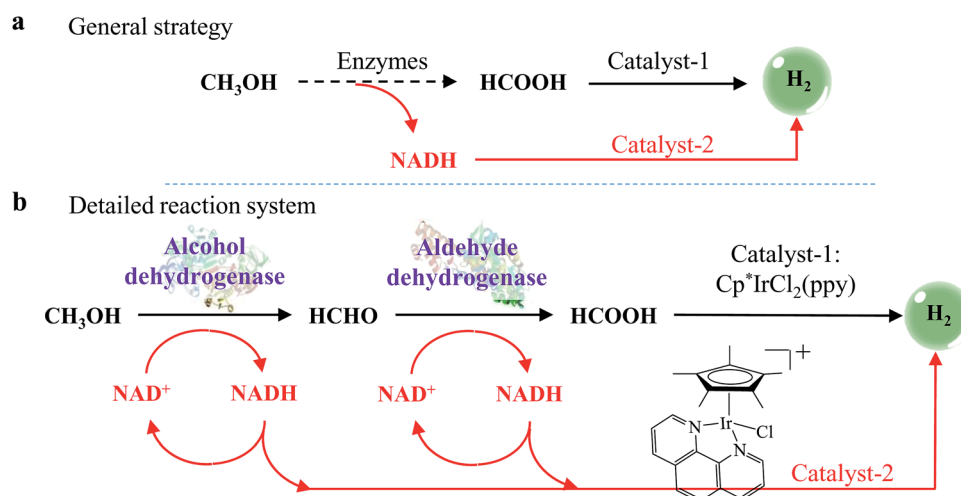
2.1. General strategy and detailed reaction system

It is well known that the methanol dehydrogenation process is extremely difficult to accomplish by chemical methods at room temperature.[24,28,29] However, formic acid dehydrogenation (reaction (4)) can be effectively catalyzed by many homogeneous and heterogeneous catalysts at near-room temperature.[17,30–37] Therefore, hydrogen production from methanol would become much easier if methanol could be first converted to formic acid.

Inspired by these ideas, we developed a general strategy to fully dehydrogenate methanol to hydrogen at near-room temperature. Scheme 1a shows that the strategy's reaction system comprises two main procedures, which are $CH_3OH \rightarrow$ HCOOH $\rightarrow H_2$ and $CH_3OH \rightarrow$ NADH $\rightarrow H_2$. In the first procedure ($CH_3OH \rightarrow$ HCOOH $\rightarrow H_2$), methanol is first dehydrogenated to formic acid by enzymes and then the formic acid is decomposed to hydrogen by catalyst-1. In the second procedure ($CH_3OH \rightarrow$ NADH $\rightarrow H_2$), NADH is generated from the dehydrogenation of methanol and then NADH is converted to hydrogen by catalyst-2. With this strategy, methanol can be fully converted to hydrogen.

$$CH_3OH + NAD^+ \xrightarrow{ADH} NADH + HCHO + H^+ \quad (6)$$

$$HCHO + H_2O + NAD^+ \xrightarrow{ALDH} NADH + HCOOH + H^+ \quad (7)$$

$$HCOOH \xrightarrow{catalyst-1} H_2 + CO_2 \quad (8)$$

$$NADH + H^+ \xrightarrow{enzyme\ mimic} NAD^+ + H_2 \quad (9)$$

Details of the reaction system's procedures ($CH_3OH \rightarrow$ HCOOH $\rightarrow H_2$ and $CH_3OH \rightarrow$ NADH $\rightarrow H_2$) are shown in Scheme 1b. In the first procedure, formic acid is generated from methanol by the cooperation of two dehydrogenation enzymes, alcohol dehydrogenase (ADH) in reaction (6) and aldehyde dehydrogenase (ALDH) in reaction (7). Then an iridium (Ir) complex catalyst decomposes the formic acid to hydrogen (reaction (8)). In the second procedure, NADH is generated from nicotinamide adenine dinucleotide (NAD^+) by the dehydrogenation of both methanol and formaldehyde (reactions (6) and (7); see Scheme 1b), and then is dehydrogenated to hydrogen by an enzyme mimic (reaction (9)). Scheme 1b also shows that NADH and NAD^+ start to cycle in the reaction system, which enables the system to work continuously. Thus, because the enzymes, the enzyme mimics, and the catalyst are all able to work at near-room temperature, the whole reaction system can produce hydrogen at near-room temperature. This near-room temperature strategy for generating hydrogen is not limited to methanol. It is also a suitable method for other organic molecules or biomass.

Scheme 1 General strategy (a) and detailed reaction system (b) for the generation of H_2 from methanol at near-room temperature. Black arrows indicate the first procedure ($CH_3OH \rightarrow$ HCOOH $\rightarrow H_2$). Red arrows indicate the second procedure ($CH_3OH \rightarrow$ NADH $\rightarrow H_2$).

As shown in Scheme 1b and reactions (6)–(9), these two main procedures are composed of 4 simple reaction steps: methanol dehydrogenation by ADH; formaldehyde dehydrogenation by ALDH; formic acid decomposition by the Ir complex; and NADH dehydrogenation by the enzyme mimics. The literature shows only a few reports for each of the steps; the entire reaction system with all four steps included has not as yet been reported. To make the whole reaction system work smoothly, the right species, such as enzymes, enzyme mimics, catalysts and so on, should be sought or synthesized. These species should work together without any obvious negative effect on each other.

2.2. The four reaction steps of the reaction system

For the first step, reaction (6), we chose ADH to perform the methanol dehydrogenation to convert methanol to formaldehyde.[38] In the meantime, NAD^+ is converted to NADH by the hydrogen deposited from methanol (Fig. S8a†). By using ADH, the most difficult reaction step in methanol reforming, i.e. methanol dehydrogenation, is successfully overcome. No oxygen is needed to partially oxidize methanol to formaldehyde.[28]

For the second step, reaction (7), we chose ALDH to perform the formaldehyde dehydrogenation to convert formaldehyde to formic acid.[38] By using a catalyst the formic acid product is very easily decomposed to hydrogen at near-room temperature.[13,15,25,26,39,40] In the meantime, NAD^+ is converted to NADH by the hydrogen deposited from formaldehyde (Fig. S8b†). An important benefit of using ADH and ALDH is that they have no negative effect on each other (Fig. S8b†).

For the third step, reaction (8), we synthesized a new polymer complex catalyst $Cp*IrCl_2(ppy)$ ($Cp*$ is 1,2,3,4,5-pentamethylcyclopentadienyl and ppy is polypyrrole), which has high activity and selectivity (the level of CO is undetectable and is << 10 ppm), to catalyze the decomposition of formic acid to hydrogen and CO_2 at near-room temperature (Fig. S9–13†). As a solid state complex catalyst, this new catalyst $Cp*IrCl_2(ppy)$ has advantages possessed by both homogeneous and heterogeneous catalysts (Fig. S10–12†).[10,11,13,15,25,26,41] In addition, the new catalyst has a uniquely high tolerance to the enzymes, coenzymes and sulfhydryl compounds (Fig. S13a†). It also has been confirmed that $[Cp*IrCl(phen)]Cl$ has no side effects on ADH and ALDH (Fig. S13b†).

For the fourth step, reaction (9), we synthesized some complex catalysts to mimic the function of hydrogenase for NADH dehydrogenation to hydrogen.[42–44] The enzyme mimics can not only directly produce H_2 from NADH (reaction (9)), but can also convert NADH back to NAD^+ (Fig. S14a†) at the same time.[45–50] The NADH and NAD^+ can then attain a cyclic reaction in the reaction system (Scheme 1b). Based on the current body of enzyme mimic research,[45–52] ours appears to be the first research to employ enzyme mimics for hydrogen production from small organic molecules (methanol).

To find highly active and compatible enzyme mimics, we synthesized a series of Ir- and Rh-complex catalysts (SI-3†). These enzyme mimics can catalyze the conversion of NADH to NAD^+ and simultaneously generate H_2 (Fig. S14a†). Compared with hydrogenase, these enzyme mimics have much higher availability and stability.[42,43] As listed in Table 1, the enzyme mimics are all catalytically active for reaction (9). Of note, however, is that only $[Cp*IrCl(phen)]Cl$ and $[Cp*IrCl(phen-NH_2)]Cl$ proved workable in the reaction mixture solution of enzymes, coenzymes and sulfhydryl compounds (Table 1 and Fig. S14b†). $[Cp*IrCl(phen)]Cl$ is also notable for having the highest compatibility (Fig. S14b†), which is due to its specific ligands with simple structures and without extra functional groups.

2.3. Hydrogen generation from methanol at near-room temperature

When we mixed the enzymes, coenzymes, catalysts and chemicals together, the four steps in the whole reaction system worked immediately and smoothly. Hydrogen was successfully produced from methanol at near-room temperature under moderate conditions and was detected by GC (Fig. 1a). This successful hydrogen production further proves the high compatibility of the species in the entire reaction system. In this process, extra amount of catalyst-1, $Cp*IrCl_2(ppy)$, and an enzyme mimic, $[Cp*IrCl(phen)]Cl$, are used to ensure the immediate conversion of HCOOH and NADH to hydrogen. Fig. 1b shows that the hydrogen production has a stable rate ($300 \ \mu mol \ h^{-1} \ kU_{(ALDH)}^{-1}$) for approximately 1900 min (~32 h), indicating that the reaction system in Scheme 1b has a long lifetime for producing hydrogen from methanol.

The activities of ADH, ALDH, catalyst-1 and catalyst-2 are calculated and listed in Table 2. We can see that the TOF of ALDH is 1120 h^{-1}, which is much higher than that of ADH, catalyst-1 and catalyst-2. Because the cost of ALDH is high, we added much higher concentrations of ADH, catalyst-1 and catalyst-2 to the reaction solution. ALDH can then work at a relatively high reaction rate and the whole reaction system can work smoothly.

According to Scheme 1, every component in the reaction system is necessary to ensure continuous hydrogen generation. To investigate the functions of the main components and be sure that each was necessary, we performed a series of control experiments. In these experiments, we studied the hydrogen generation in the absence of each main component in turn.

As shown in Fig. 1c, no hydrogen was detected in the absence of ADH (Fig. 1c, black curve), indicating that methanol dehydrogenation is the most important step for hydrogen

Table 1 Activities and compatibilities of hydrogenase mimics for hydrogen production from NADH

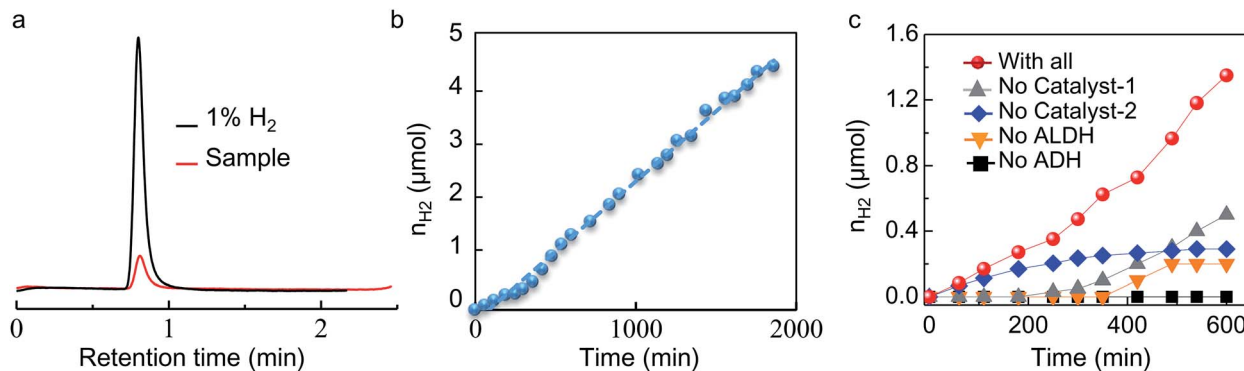| Entry	Catalyst-2	TOF (h^{-1})	Compatibility
1	$[Cp*IrCl(phen-NO_2)]Cl$	6.29	No
2	$[Cp*IrCl(phen-NH_2)]Cl$	3.63	High
3	$[Cp*RhCl(phen-NO_2)]Cl$	3.06	No
4	$[Cp*RhCl(bpym)]Cl$	3.03	No
5	$[Cp*IrCl(phen)]Cl$	2.39	High
6	$[\{Ir(Cp*)(Cl)\}_2(bpym)]Cl_2$	2.39	No
7	$[Cp*IrCl(bpym)]Cl$	0.33	No

Fig. 1 H_2 generation from methanol at 30 °C. (a) Hydrogen measurement by gas chromatography (GC). (b) Hydrogen generation from methanol for about 1900 min at pH 8.05. The H_2 generation rate is 300 μmol h^{-1} kU$_{(ALDH)}$$^{-1}$ (refer to part 2.4 for the definition of kU$_{(ALDH)}$). (c) H_2 generation from methanol in the absence of one component. Basic conditions for the reaction solution with all components: 5.0 mL phosphate buffer (pH = 8.05) containing 400 mM CH$_3$OH, 4 mg catalyst-1 (Cp*IrCl$_2$(ppy)), 500 μM catalyst-2 ([Cp*IrCl(phen)]Cl), 1 mM NAD$^+$, 0.5 U ALDH and 30 U ADH in an N_2 atmosphere.

generation. Scheme 1 shows that methanol dehydrogenation by ADH is the first step of all the reactions. If methanol cannot be converted to formaldehyde and NADH by ADH, it is impossible for the following reaction steps to occur (Scheme 1). This means that the whole reaction system will fail to generate any hydrogen in the absence of ADH (Fig. 1c, black curve).

With ALDH absent, no hydrogen was generated in the initial 350 minutes (Fig. 1c, orange curve). After 350 minutes, trace hydrogen could be detected by GC and its concentration increased slowly with time (Fig. 1c, orange curve). After 500 minutes, the hydrogen concentration stopped increasing. Scheme 1 shows that HCOOH cannot be generated from HCHO and HCHO accumulates in the solution due to the absence of ALDH. The hydrogen from HCOOH cannot be accessed; it can only be generated from NADH, which is produced by methanol dehydrogenation. As soon as the HCHO reaches an equilibrium concentration, the whole reaction system stops working, causing the hydrogen concentration to stop increasing (Fig. 1c, orange curve).

When catalyst-1 was missing, no hydrogen was generated in the initial 200 minutes (Fig. 1c, grey curve). After 200 minutes, the hydrogen concentration increased slowly with time (Fig. 1c, grey curve). Scheme 1 shows that in the absence of catalyst-1, hydrogen is only generated through NADH. Compared to the solution lacking ALDH (Fig. 1c, orange curve), more NADH was generated through this process, and consequently more hydrogen was generated (Fig. 1c, grey curve).

In the absence of catalyst-2, the amount of hydrogen increased with time from the start of the process, but stopped increasing after about 400 minutes (Fig. 1c, blue curve). Scheme 1 shows that in the absence of catalyst-2, hydrogen is only generated through formic acid dehydrogenation. NADH accumulates in the reaction solution, and because the NADH cannot be converted back to NAD$^+$ fast enough, the formic acid formation rate decreases. Consequently, the hydrogen generation rate decreases with time (Fig. 1c, blue curve). As soon as the NADH and NAD$^+$ reach equilibrium concentrations, the methanol and formaldehyde dehydrogenation stop, and consequently, hydrogen generation stops.

2.4. The effect of pH on the hydrogen generation rate

To investigate the effect of pH on the reaction, we produced hydrogen from methanol at different pH values. Fig. 2a shows the hydrogen production and generation rate during methanol–water reforming at pH values from 7.00 to 8.25. At each pH, hydrogen production linearly increases with time, however, the slopes of the curves for the various pH values are very different, indicating different hydrogen generation rates. Fig. 2b shows that the optimal pH is 7.90, at which the hydrogen generation rate reaches a maximum value of 672 μmol h^{-1} kU$_{(ALDH)}$$^{-1}$, indicating that 672 μmol hydrogen could be generated per hour per kilo of active unit (kU) of ALDH. One unit (U) is defined as the amount of the enzyme that catalyzes the conversion of 1 μmol of substrate per minute. For example, one unit of ADH can

Table 2 TOF and concentrations under different conditions

| Figure	TOF/concentration	ADH	ALDH	Catalyst-1 (Cp*IrCl$_2$(ppy))	Catalyst-2 ([Cp*IrCl(phen)]Cl)
Fig. 1b	TOF (h^{-1})	270	1120	0.17	0.06
Fig. 1b	Concentration	1.11×10^{-7} M	2.67×10^{-8} M	0.8 mg mL^{-1}	5×10^{-4} M
Fig. 2b	TOF at pH = 7.90 (h^{-1})	605	2510	0.38	0.14
Fig. 2b	Concentration at pH = 7.90	1.11×10^{-7} M	2.67×10^{-8} M	0.8 mg mL^{-1}	5×10^{-4} M
Fig. 2c–f	Maximum TOF (h^{-1})	220	947	310	9.61
Fig. 2c–f	Concentration at maximum TOF	8.91×10^{-8} M	3.37×10^{-7} M	0.5 mg mL^{-1}	2×10^{-5} M
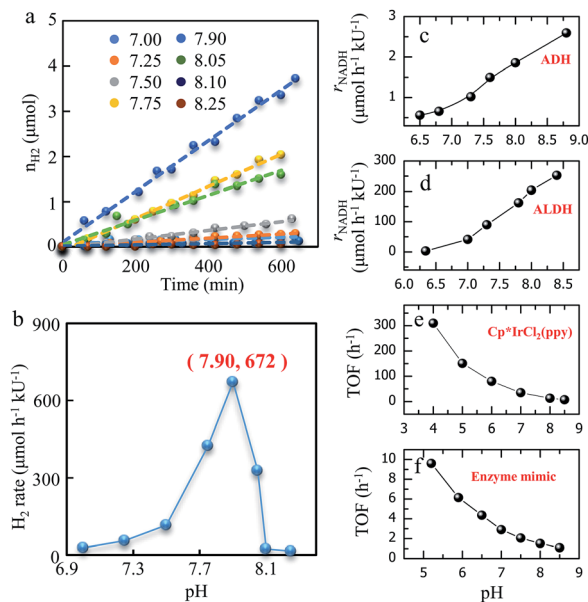
Fig. 2 Effect of pH on H_2 generation from methanol. (a) H_2 generation at different pH values. Conditions: 5.0 mL phosphate buffer containing 400 mM CH_3OH, 500 μM [Cp*IrCl(phen)]Cl, 1 mM NAD^+, 4 mg Cp*IrCl$_2$(ppy), 0.5 U ALDH and 30 U ADH at 30 °C. kU is used for ALDH. (b) H_2 generation rate at the different pH values in (a). (c) The pH dependent activity of ADH for CH_3OH dehydrogenation. kU is for ADH. (d) The pH dependent activity of ALDH for HCHO dehydrogenation. kU is for ALDH. (e) The pH dependent activity of catalyst-1 (Cp*IrCl$_2$(ppy)) for HCOOH dehydrogenation. (f) The pH dependent activity of the enzyme mimic ([Cp*IrCl(phen)]Cl) for NADH dehydrogenation. Refer to SI-4 for the detailed conditions.†

convert 1.0 μmol of ethanol to acetaldehyde per min at pH 8.8 at 25 °C; one unit of ALDH can oxidize 1.0 μmol of acetaldehyde to acetic acid per min at pH 8.0 at 25 °C in the presence of NAD^+.

The optimal pH is due to the different effects the pH on the activity of the enzymes, catalysts and enzyme mimics. Fig. 2c and d show that the activities of ADH and ALDH increase with the increase of the pH of the solution, which is in accordance with the ADH information provided by Sigma-Aldrich Co. LLC. Fig. 2e and f show that the activities of catalyst-1 (Cp*IrCl$_2$(ppy)) and catalyst-2 (enzyme mimic [Cp*IrCl(phen)]Cl) increase with decreasing pH, which is consistent with results in the literature.[47] Therefore, the activity of ADH and ALDH compete with that of catalyst-1 and catalyst-2 when the pH increases, until an optimum pH of 7.90 is obtained. To reduce the negative effect of the low activities of catalyst-1 and catalyst-2 at high pH values, we used larger amounts of catalyst-1 and catalyst-2 to compensate for their lower activity. Since catalyst-1 and catalyst-2 are synthesized artificially, they have the advantages of higher stability and lower cost in comparison with enzymes.

Table 2 shows that the maximum activities of catalyst-1 and catalyst-2 in Fig. 2e and f are much higher than that in Fig. 2b. For example, the maximum activity of catalyst-1 in Fig. 2e is 310 h^{-1}, which is much higher than 0.38 h^{-1} in Fig. 2b. This is because the working conditions, such as the reactant concentration and pH value, are better in the experiments shown in Fig. 2e and f than in those shown in Fig. 2b. However, Table 2

shows that the activities of ADH and ALDH in Fig. 2c and d are much lower than those in Fig. 2b. For example, the maximum activity of ADH in Fig. 2c is 220 h^{-1}, which is much lower than 605 h^{-1} in Fig. 2b. This is mainly due to the low concentration of NAD^+ in the experiments shown in Fig. 2c and d compared to that in the experiments shown in Fig. 2b. In addition, due to the synergistic effect of ADH, ALDH, catalyst-1 and catalyst-2, the enzymes (ADH and ALDH) can exhibit higher activities in the mixture solution. The synergistic effect is mainly due to the immediate removal of HCHO by cooperation of the four catalysts, since we found that a high concentration of HCHO is poisonous to both ADH and ALDH. Fig. S8† shows that the initial reaction rate for the reaction solution with both ADH and ALDH is higher than that with only ADH or ALDH.

Therefore, the reaction rate of the whole reaction system has a high potential for improvement if ADH and ALDH have higher activities. In the current work, the hydrogen generation rate is mainly limited by the low activities of ADH and ALDH because the ADH and ALDH used are the commercially available ones from Sigma-Aldrich that have not yet been optimized. In future work, the hydrogen generation rate may increase through enzyme engineering to improve the activities of ADH and ALDH specifically for methanol and formaldehyde dehydrogenation, respectively.

3. Conclusions

In summary, we successfully designed a strategy to fully convert methanol to hydrogen at near-room temperature without any assistance from extra energy or consumptive additives. The strategy involves two procedures, which are $CH_3OH \rightarrow HCOOH \rightarrow H_2$ and $CH_3OH \rightarrow NADH \rightarrow H_2$. Importantly, this research discovered an enzyme mimic, [Cp*IrCl(phen)]Cl, which can continuously generate hydrogen from NADH at near-room temperature and which is highly compatible with the enzymes, coenzymes and enzyme inhibitors. This research also reveals that the hydrogen generation rate can be strongly affected by the reaction pH. The lifetime measurement shows that hydrogen can be continuously generated with a constant production rate (300 μmol h^{-1} kU$_{(ALDH)}^{-1}$) for 1900 min (∼32 h). The strategy and catalysts created in this research can also be applied to hydrogen production from other small organic molecules (e.g. ethanol and ethylene glycol) or biomass (e.g. glucose, starch and cellulose).

Conflicts of interest

There are no conflicts of interest to declare.

Acknowledgements

bionics (Y3AAA11004) and the Thousand Youth Talents Plan (Y3BQA11001).

References

1 A. Monney, E. Barsch, P. Sponholz, H. Junge, R. Ludwig and M. Beller, *Chem. Commun.*, 2014, **50**, 707–709.

2 J. Kothandaraman, A. Goeppert, M. Czaun, G. A. Olah and G. K. S. Prakash, *J. Am. Chem. Soc.*, 2016, **138**, 778–781.

3 M. Trincado, D. Banerjee and H. Gruetzmacher, *Energy Environ. Sci.*, 2014, **7**, 2464–2503.

4 K. Sordakis, A. Tsurusaki, M. Iguchi, H. Kawanami, Y. Himeda and G. Laurenczy, *Green Chem.*, 2017, **19**, 2371–2378.

5 A. Tsurusaki, K. Murata, N. Onishi, K. Sordakis, G. Laurenczy and Y. Himeda, *ACS Catal.*, 2017, **7**, 1123–1131.

6 J. Liu, J. Cao, Q. Huang, X. Li, Z. Zou and H. Yang, *J. Power Sources*, 2008, **175**, 159–165.

7 R. E. Rodriguez-Lugo, M. Trincado, M. Vogt, F. Tewes, G. Santiso-Quinones and H. Gruetzmacher, *Nat. Chem.*, 2013, **5**, 342–347.

8 E. A. Bielinski, M. Förster, Y. Zhang, W. H. Bernskoetter, N. Hazari and M. C. Holthausen, *ACS Catal.*, 2015, **5**, 2404–2415.

9 K.-I. Fujita, R. Kawahara, T. Aikawa and R. Yamaguchi, *Angew. Chem., Int. Ed.*, 2015, **54**, 9057–9060.

10 D. R. Palo, R. A. Dagle and J. D. Holladay, *Chem. Rev.*, 2007, **107**, 3992–4021.

11 R. González-Gil, C. Herrera, M. Á. Larrubia, P. Kowalik, I. S. Pieta and L. J. Alemany, *Int. J. Hydrogen Energy*, 2016, **41**, 19781–19788.

12 F. Wang and G. Wang, *Int. J. Hydrogen Energy*, 2016, **41**, 16835–16841.

13 F. Ahmadi, M. Haghighi and H. Ajamein, *J. Mol. Catal. A: Chem.*, 2016, **421**, 196–208.

14 T. Suenobu, Y. Isaka, S. Shibata and S. Fukuzumi, *Chem. Commun.*, 2015, **51**, 1670–1672.

15 M. Trincado, V. Sinha, R. E. Rodriguez-Lugo, B. Pribanic, B. de Bruin and H. Gruetzmacher, *Nat. Commun.*, 2017, **8**, 14990.

16 S. Fukuzumi, T. Kobayashi and T. Suenobu, *J. Am. Chem. Soc.*, 2010, **132**, 1496–1497.

17 J. F. Hull, Y. Himeda, W.-H. Wang, B. Hashiguchi, R. Periana, D. J. Szalda, J. T. Muckerman and E. Fujita, *Nat. Chem.*, 2012, **4**, 383–388.

18 Y. Im, S. Kang, K. M. Kim, T. Ju, G. B. Han, N. K. Park, T. J. Lee and M. Kang, *Int. J. Photoenergy*, 2013, **2013**, 452542.

19 L. E. Heim, S. Vallazza, D. van der Waals and M. H. G. Prechtl, *Green Chem.*, 2016, **18**, 1469–1474.

20 X. Yang, *ACS Catal.*, 2014, **4**, 1129–1133.

21 J. Campos, L. S. Sharninghausen, M. G. Manas and R. H. Crabtree, *Inorg. Chem.*, 2015, **54**, 5079–5084.

22 A. Naldoni, M. D'Arienzo, M. Altomare, M. Marelli, R. Scotti, F. Morazzoni, E. Selli and V. Dal Santo, *Appl. Catal., B*, 2013, **130**, 239–248.

23 Y.-L. Zhan, Y.-B. Shen, S.-P. Li, B.-H. Yue and X.-C. Zhou, *Chin. Chem. Lett.*, 2017, **28**, 1353–1357.

24 M. Nielsen, E. Alberico, W. Baumann, H.-J. Drexler, H. Junge, S. Gladiali and M. Beller, *Nature*, 2013, **495**, 85–89.

25 E. Alberico, P. Sponholz, C. Cordes, M. Nielsen, H. J. Drexler, W. Baumann, H. Junge and M. Beller, *Angew. Chem., Int. Ed.*, 2013, **52**, 14162–14166.

26 P. Hu, Y. Diskin-Posner, Y. Ben-David and D. Milstein, *ACS Catal.*, 2014, **4**, 2649–2652.

27 E. Alberico, A. J. J. Lennox, L. K. Vogt, H. Jiao, W. Baumann, H.-J. Drexler, M. Nielsen, A. Spannenberg, M. P. Checinski, H. Junge and M. Beller, *J. Am. Chem. Soc.*, 2016, **138**, 14890–14904.

28 L. E. Heim, D. Thiel, C. Gedig, J. Deska and M. H. G. Prechtl, *Angew. Chem., Int. Ed.*, 2015, **54**, 10308–10312.

29 M. Anderez-Fernandez, L. K. Vogt, S. Fischer, W. Zhou, H. Jiao, M. Garbe, S. Elangovan, K. Junge, H. Junge, R. Ludwig and M. Beller, *Angew. Chem., Int. Ed.*, 2017, **56**, 559–562.

30 W. Wang, T. He, X. Liu, W. He, H. Cong, Y. Shen, L. Yan, X. Zhang, J. Zhang and X. Zhou, *ACS Appl. Mater. Interfaces*, 2016, **8**, 20839–20848.

31 Y. Himeda, S. Miyazawa and T. Hirose, *Chemsuschem*, 2011, **4**, 487–493.

32 P. G. Alsabeh, D. Mellmann, H. Junge and M. Beller, Ruthenium-Catalyzed Hydrogen Generation from Alcohols and Formic Acid, Including Ru-Pincer-Type Complexes, in *Ruthenium in Catalysis*, ed. C. Bruneau and P. H. Dixneuf, Springer International Publishing, 2014, vol. 48, pp. 45–79.

33 D. Mellmann, E. Barsch, M. Bauer, K. Grabow, A. Boddien, A. Kammer, P. Sponholz, U. Bentrup, R. Jackstell, H. Junge, G. Laurenczy, R. Ludwig and M. Beller, *Chem.–Eur. J.*, 2014, **20**, 13589–13602.

34 M. Montandon-Clerc, A. F. Dalebrook and G. Laurenczy, *J. Catal.*, 2016, **343**, 62–67.

35 T. Zell and D. Milstein, *Acc. Chem. Res.*, 2015, **48**, 1979–1994.

36 M. Czaun, J. Kothandaraman, A. Goeppert, B. Yang, S. Greenberg, R. B. May, G. A. Olah and G. K. S. Prakash, *ACS Catal.*, 2016, **6**, 7475–7484.

37 D. Jantke, L. Pardatscher, M. Drees, M. Cokoja, W. A. Herrmann and F. E. Kuehn, *Chemsuschem*, 2016, **9**, 2849–2854.

38 J. Canivet, G. Süss-Fink and P. Štěpnička, *Eur. J. Inorg. Chem.*, 2007, **2007**, 4736–4742.

39 G. Papp, G. Olveti, H. Horvath, A. Katho and F. Joo, *Dalton Trans.*, 2016, **45**, 14516–14519.

40 C. Guan, D.-D. Zhang, Y. Pan, M. Iguchi, M. J. Ajitha, J. Hu, H. Li, C. Yao, M.-H. Huang, S. Ming, J. Zheng, Y. Himeda, H. Kawanami and K.-W. Huang, *Inorg. Chem.*, 2017, **56**, 438–445.

41 D. Mellmann, P. Sponholz, H. Junge and M. Beller, *Chem. Soc. Rev.*, 2016, **45**, 3954–3988.

42 H. O. Wolfgang Lubitz, O. Rüdiger and E. Reijerse, *Chem. Rev.*, 2014, **114**, 4081–4148.

43 D. Schilter, J. M. Camara, M. T. Huynh, S. Hammes-Schiffer and T. B. Rauchfuss, *Chem. Rev.*, 2016, **116**, 8693–8749.

44 S. Fukuzumi and T. Suenobu, *Dalton Trans.*, 2013, **42**, 18–28.

45 R. Becker, S. Amirjalayer, P. Li, S. Woutersen and J. N. H. Reek, *Sci. Adv.*, 2016, **2**, e1501014.

46 S. Betanzoslara, Z. Liu, A. Habtemariam, A. M. Pizarro, B. Qamar and P. J. Sadler, *Angew. Chem., Int. Ed.*, 2012, **51**, 3897–3900.

47 Y. Maenaka, T. Suenobu and S. Fukuzumi, *J. Am. Chem. Soc.*, 2012, **134**, 367–374.

48 J. Vijaya Sundar and V. Subramanian, *Organometallics*, 2012, **31**, 8525–8536.

49 H. Wu, C. Tian, X. Song, C. Liu, D. Yang and Z. Jiang, *Green Chem.*, 2013, **15**, 1773–1789.

50 X. Wang and H. H. P. Yiu, *ACS Catal.*, 2016, **6**, 1880–1886.

51 H. Yoon, Y.-M. Lee, W. Nam and S. Fukuzumi, *Chem. Commun.*, 2014, **50**, 12944–12946.

52 Y. Maenaka, T. Suenobu and S. Fukuzumi, *J. Am. Chem. Soc.*, 2012, **134**, 9417–9427.